Complexes between C-Reactive Protein and Very Low Density Lipoprotein Delay Bacterial Clearance in Sepsis

Zhenxing Cheng,* Simon T. Abrams,[†] Julien Toh,[‡] Susan S. Wang,[§] Colin Downey,[¶] Xiaoling Ge,[†] Qian Yu,* Weiping Yu,* Guozheng Wang,*[,†] and Cheng-Hock Toh[†,¶]

C-reactive protein (CRP) can increase up to 1000-fold in blood and form complexes with very low density lipoproteins (VLDL). These complexes are associated with worse outcomes for septic patients, and this suggests a potential pathological role in sepsis. Complex formation is heightened when CRP is over 200 mg/l and levels are associated with the severity of sepsis and blood bacterial culture positivity. Using a mouse bacteremia model, blood bacterial clearance can be delayed by i.v. injection of CRP–VLDL complexes. Complexes are more efficiently taken up by activated U937 cells in vitro and Kupffer cells in vivo than VLDL alone. Both in vitro–generated and naturally occurring CRP–VLDL complexes reduce phagocytosis of bacteria by activated U937 cells. Fcγ and scavenger receptors are involved and a competitive mechanism for clearance of CRP–VLDL complexes and bacteria is demonstrated. Interaction of phosphocholine groups on VLDL with CRP is the major driver for complex formation and phosphocholine can disrupt the complexes to reverse their inhibitory effects on phagocytosis and bacterial clearance. Increased formation of CRP–VLDL complexes is therefore harmful and could be a novel target for therapy in sepsis. *The Journal of Immunology*, 2020, 204: 000–000.

C-reactive protein (CRP) is an acute phase protein, with concentrations increasing by up to 1000-fold in sepsis, to reach circulation levels of 500 mg/l (1) in circulation, and is used as a diagnostic marker of sepsis (2). High CRP levels are associated with poor disease outcomes, but the precise mechanism is poorly understood (3, 4). Although poor clinical outcomes are related to the severity of the underlying disease, there remains controversy as to whether CRP plays a protective or harmful role. The majority of reports have considered CRP as protective because CRP is involved in the innate immune response to activate complement, opsonize pathogens as well as damaged cells, and cellular breakdown products (5, 6). However, CRP has been implicated in the development of atherosclerosis and is regarded as a risk factor for cardiovascular diseases (7–9). CRP can enlarge the infarct size in a rat model for acute myocardial infarction, and this enlargement is associated with complement activation (10). Another study has claimed that CRP has no protective effect on mice challenged with LPS and that very high CRP levels are associated with poor outcome (11). High CRP levels in CRP-transgenic mice also cause endothelial dysfunction (12). These observations suggest that CRP has dual effects, both protective and harmful, depending on individual circumstances.

CRP is a calcium-binding protein that exists as a pentamer under physiological buffer conditions. Phosphocholine (Pch) is the natural ligand of CRP (13), with CRP binding to apoptotic cells and certain bacterial strains through this group (5). CRP also binds oxidized low-density lipoprotein through oxidized phosphatidylcholine (14), and this interaction increases oxidized low-density lipoprotein uptake by macrophages (15). Interactions between CRP and very low density lipoprotein (VLDL) has been recognized for over two decades (16–18) and is demonstrated in humans when acute phase serum containing high CRP levels is incubated with serum from patients with type III to V hyperlipoproteinemia (18). No physiological function has been ascribed to the complex. However, our chance identification of the CRP–VLDL complex in patients with sepsis by a different clinical investigative route may provide relevant insight into its function. When the activated partial thromboplastin time (aPTT) coagulation assay was performed, using an automated optical analyzer, a phenomenon described as the biphasic waveform was observed (19). This finding is associated with sepsis and disseminated intracellular coagulation (20) and is caused by interference with

*Medical School, Southeast University, Nanjing 210009, China; [†]Institute of Infection and Global Health, University of Liverpool, Liverpool L69 7BE, United Kingdom; [‡]Wirral University Teaching Hospital NHS Foundation Trust, Upton, Wirral CH49 5PE, United Kingdom; [§]Royal London Hospital, Whitechapel, London E1 1FR, United Kingdom; and [¶]Royal Liverpool University Hospital, University of Liverpool, Liverpool L7 8XP, United Kingdom

ORCIDs: 0000-0003-0847-2582 (Z.C.); 0000-0003-3262-7847 (J.T.); 0000-0002-7047-9403 (X.G.).

Address correspondence and reprint requests to Prof. Weiping Yu, Prof. Cheng-Hock Toh, or Prof. Guozheng Wang, Medical School, Southeast University, Nanjing 210009, China (W.Y.), Royal Liverpool University Hospital, University of Liverpool, Liverpool L7, 8XP, U.K. (C.-H.T.), or Institute of Infection and Global Health, University of Liverpool, Liverpool L69 7BE, U.K. (G.W.). Email addresses: yuweiping@seu.edu.cn (W.Y.), toh@liverpool.ac.uk (C.-H.T.), or wangg@liverpool.ac.uk (G.W.)

light transmittance due to increased formation of calcium-dependent CRP–VLDL complexes (21). This result has now been validated as a reliable indicator of poor outcome in sepsis (22–24). These observations suggest that the CRP–VLDL complex may be a pathological factor in diseases associated with high CRP levels.

Phagocytosis of CRP-opsonized particles, bacteria, and cells occurs through Fcγ I and II receptors (25). These are highly expressed on macrophages as scavenger receptors and are the major receptors for clearing modified or aggregated lipoproteins (26–28). These receptors could therefore be involved in the clearance of CRP–VLDL complexes, and we hypothesize that the phagocytic function of macrophages and blood bacterial clearance in sepsis may be affected if large amounts of CRP–VLDL complexes are present. In this study, we have established an ELISA to directly quantify circulating CRP–VLDL complexes. We have found that levels of these complexes in blood were associated with the severity of sepsis and the positivity of blood bacterial culture. Using a mouse bacteremia model, we also find that CRP–VLDL complexes significantly delayed blood bacterial clearance, which may result from their competitive inhibitory effect on the phagocytic function of macrophages. Pch, the head group of phosphatidylcholine, is able to efficiently disrupt CRP–VLDL complexes and reverse the inhibitory effects on bacterial phagocytosis in vitro and blood bacterial clearance in vivo. Therefore, we speculate that the CRP–VLDL complex could have potential as a diagnostically-linkable target for new therapies in sepsis.

Materials and Methods
Patients

Study samples (citrated plasma and serum) were from patients on the general intensive care unit (ICU) at the Royal Liverpool University Hospital, Liverpool, U.K., diagnosed with severe sepsis and septic shock as defined by the American College of Chest Physicians/Society for Critical Care Medicine Consensus Conference Committee (29). This was in accordance with protocol approved by the Local Research Ethics Committee (Ref: 07/H1009/64 and 07/H1005/124) and University sponsorship (Ref: UoL000298), including the recruitment of controls (Ref: RETH000685). In 2016, the American College of Chest Physicians/Society for Critical Care Medicine Consensus Conference Committee redefined sepsis and we have re-examined the clinical records and found that all patients recruited before 2016 also matched the new sepsis-3 criteria. The demographics of patients are shown in Supplemental Table I.

Reagents

VLDL, low density lipoprotein (LDL), high density lipoprotein, CRP (Merck); Pch (TCI Europe); anti-CRP, anti-ApoB (AbD Serotec; Sigma-Aldrich; Santa Cruz Biotechnology); anti-CD32, CD64, and CD36 (AbD Serotec); and anti– scavenger receptor A1 (SA1) (R&D Systems) Abs were purchased. VLDL was isolated from human or mouse serum by ultracentrifugation, and CRP was isolated from human ascites (07/H1005/124) using immobilized p-aminophenyl phosphoryl choline (Pierce) and gel filtration were monitored using E-TOXATE (Sigma-Aldrich) for LPS contamination to reach over 95% purity and no detectable LPS. In vitro–generated CRP–VLDL complexes were prepared by mixing CRP with VLDL at 1:5 (w/w of protein) ratio in 2.5 mM CaCl$_2$, which was optimized by gel filtration and monitored by turbidity assay.

Measuring CRP–VLDL complexes using ELISA. Assay design

Immobilization of CRP–VLDL complexes can be achieved using anti-CRP or ApoB Abs. We have tried both types of assays and found that serum with very high CRP levels can saturate the CRP binding sites with non-complexed CRP and thereby mask the real level of CRP–VLDL complexes. In contrast, the circulating levels of VLDL and LDL fluctuate much less than that of CRP, and using ApoB-coated plates was more appropriate and accurate. In brief, procedures were as follows: 1:50–1:100 serum dilution and anti-CRP-HRP (Abcam, Cambridge, U.K.) 1:12,000 dilution were used with modified HEPES wash buffer containing 2.5 mM CaCl$_2$ on anti-ApoB–coated plates. In brief, 8 μg/ml ApoB (AbD Serotec) was coated on ELISA plates. After blocking with blocking buffer (5% dry milk in buffer A: 20 mM HEPES [pH 7.4], 100 mM NaCl, 2.5 mM CaCl$_2$), the

plates were incubated with the 1:20–1:100 diluted serum in buffer B (1% dry milk in buffer A) at room temperature (20–22°C) for 3 h. After extensive washing with buffer B, the plates were incubated with 1:10,000 diluted anti-CRP-HRP in buffer B at room temperature for 1 h and then washed. The chromogen was added and incubated for 15 min and stopped by adding stop buffer: 0.5 M H$_2$SO$_4$, OD450 nm was measured by a plate reader. The standard curves were first produced using fresh in vitro–generated CRP–VLDL complexes as mentioned above. The amount of CRP–VLDL complexes were represented by the concentration of ApoB in the complexes. Generation of standard curves was as follows: in vitro–generated CRP–VLDL complexes were used to generate a standard curve. The amount of ApoB that complexed with CRP was determined using an anti-CRP coated plate with a standard curve generated at the same time using a commercial ApoB kit. The CRP–VLDL standard curve was then generated by diluting the in vitro–generated CRP–VLDL complexes with a known concentration of complexed ApoB. With this standard curve, the concentrations of CRP–VLDL complexes in sera from normal and patients were determined. Sera with very high levels of CRP–VLDL complexes were selected and pooled. After determining the concentration of CRP–VLDL complexes, the pooled serum was aliquoted and stored at −80°C. For each assay, the standard curve was generated through a serial dilution of this pooled serum with known CRP–VLDL concentration. Complexes in this serum are very stable, at least within a 6 mo period.

aPTT waveform analysis

aPTT waveform analysis was carried out as described in our previous publication (20). As with previous studies, transmittance level at 18 s (TL18) was used to quantify the abnormality (<99%), with normal values ≥99%.

Mutant CRP proteins

Two mutant CRP proteins were prepared using pET16 (b+) vector (30) with His-tag removed by factor Xa (Qiagen). Gel filtration ensured mutant CRP purity (>99%) and that CRP was in pentameric form. T173A mutant protein was produced as previously described (25).

VLDL and CRP–VLDL uptake

VLDL labeled with Na [^{125}I] using precoated iodination tubes (Pierce) to achieve 100–200 cpm/ng protein was mixed with VLDL-depleted serum (1:2). After centrifugation (14,000 rpm, 5 min), one part of the supernatant was mixed with CRP and the other with an equal volume of buffer. Activated U937 cells (using PMA) were incubated with 80 μl basal medium (without serum), 30 μl mixture (with or without CRP), and 10 μl buffer or blocking Abs in duplicate 96-well plates, one at 4°C and the other at 37°C for 4 h. After washing with cold PBS, lysed cells (using 0.1 M NaOH) were γ-counted and total protein was measured. VLDL uptake = VLDL protein/total cell protein at 37°C – that at 4°C.

Bacteria clearance assay

C57/BL male mice of average weight (∼22 g) from the Shanghai Laboratory Animal Center/Experimental Animal Centre (Shanghai, China) were kept at the Research Centre of Gene Modified Mice, State Education Ministry Laboratory of Developmental Genes and Human Diseases, Southeast University, Nanjing, China. All procedures performed according to state laws under the license (Jiangsu province, 2151981) and were monitored by local inspectors. To reduce contamination, BL21 was transfected with pET16(b+) to gain resistance to ampicillin and then injected into tail veins. To allow bacterial adaptation to the mouse environment, the cycle of injection–culture–injection was repeated three times prior to formal experiments. Freshly cultured bacteria were suspended in saline, and the amount equal to ∼50,000 CFU/ml blood at 5 min after injection was given through a tail vein to each mouse. Twenty microliters of blood was taken through different veins using heparinized needles/tubes at different time points and cultured.

Immunohistofluorescent staining

Male C57/BL mice were injected with fluorescent BL21 bacteria, 1 × 10^5/mouse, or 200 μl (∼0.5 mg) of FITC-labeled VLDL with or without CRP. After 4 h, mice were euthanized and liver/spleen fixed with 4% (w/v) paraformaldehyde for 24 h, then stored in 70% (v/v) ethanol prior to embedding. For staining, 7-μm slices were dewaxed and permeabilized. After blocking with goat serum (Sigma-Aldrich), anti-CD163 Ab (1:50 dilution; Santa Cruz Biotechnology) and anti-goat IgG TRICT conjugate (1:100 dilution; Sigma-Aldrich) were used. Bacteria (green) or VLDL (green) and Kupffer cells (red) were imaged with an LSM 510 Zeiss confocal microscope.

Phagocytosis assay

Escherichia coli, *BL21* (Novagen) transformed with pET16b-GFP (>99% fluorescent) was incubated with PMA-activated U937 cells (20:1 ratio) at 37°C for 1 h and extensively washed. Cells detached by 0.02% EGTA were analyzed using a FACScan flow cytometer (BD Sciences). Percentage of fluorescent cells was calculated using CellQuest software. Because flow cytometry could not distinguish phagocytic events from bacterial associations, a modified phagocytosis assay using eight-well chamber slides was used. After extensive washing, cells fixed with 4% (w/v) paraformaldehyde were stained with 10 μg/ml propidium iodide. Bacteria (green) and nuclei (red) were counted under a fluorescent microscope (100× objective, 10–20 fields for >200 cells). Phagocytic index, the average bacteria/nucleus, was calculated. To validate the methodology, confocal microscopy was used to reconstitute the three-dimensional image of cells and fluorescent bacteria, demonstrating that over 95% of the bacteria were within the cells (data not shown).

Statistical analysis

The differences in outcomes between two groups and more than two groups were assessed using Student *t* test and ANOVA with Bonferroni correction, respectively. In those data that were not normally distributed, median regression were performed. To assess differences in bacterial clearance, we used the time taken to reach bacterial clearance in each mouse model as our outcome using negative binomial regression models.

Results

The levels of circulating CRP–VLDL complexes are associated with the severity of sepsis and blood bacterial culture positivity

The aPTT biphasic waveform reflects formation of CRP–VLDL complexes through a recalcification process at a calcium concentration of ~8 mM. Evidence for their existence in vivo at physiological calcium concentrations have been demonstrated previously (21), but the development of an ELISA has now enabled us to quantify their circulating levels. Using serum samples, CRP–VLDL complexes were detectable in patients with sepsis but not in healthy donors (Fig. 1A). About 70% of the complexes could be disrupted by adding 5 mM EGTA (Fig. 1A), indicating the complexes are calcium dependent. Further evaluation in 67 patients from the ICU showed that levels of CRP–VLDL complexes were associated with the severity of sepsis (Fig. 1B). Patients with septic shock had significantly higher levels (median 103.8 mg/l, interquartile range [IQR] 65.7, 165.6; $n = 25$) than those without shock (median 32.9 mg/l, IQR 21.5, 82.5; $n = 21$), nonseptic ICU patients (median 17.9 mg/l, IQR 7.8, 25.8; $n = 21$), and healthy donors (median 1.1 mg/l, IQR 0, 4.32; $n = 20$) (median regression, $p < 0.01$) (Fig. 1B). Interestingly, complex levels were also significantly higher in septic patients with positive blood bacterial cultures (median 111.7 mg/l, IQR 37.5, 167.7; $n = 28$) than those who were negative (49.5 mg/l, IQR 23.4, 75.7; $n = 18$) ($p < 0.05$) (Fig. 1C), suggesting that high levels of circulating CRP–VLDL complexes may affect blood bacterial clearance.

CRP–VLDL complexes delay bacterial clearance in a mouse model of bacteremia

To examine if CRP–VLDL complexes could impair blood bacterial clearance, i.v. injection of BL21, a disabled *E. coli* strain, at 10^7 CFU/mouse per injection was used with no detectable adverse effect, and no mice died up to 120 h after injection. When 6×10^4 BL21 bacteria were injected, ~5×10^4 CFU/ml were found circulating in the blood after 5 min. No living bacteria were detected in any mouse blood taken at 48 h (Fig. 2A, Supplemental Table II). Coinfusion of in vitro–generated human CRP–VLDL complexes (containing 40 μg CRP + 200 μg Apo protein/20 g body weight [b.w.]) significantly delayed the bacterial clearance by a factor of 2.1 compared with bacteria alone (incidence rate ratio [IRR] 2.13: 95% CI; 1.65, 2.73), but no significant effect was observed when coinfused with VLDL (200 μg protein/20 g b.w.)

(IRR 1.25: 95% CI; 0.96, 1.63). The effect of CRP–VLDL complexes became most apparent at 4 h postinjection with about only 50% of injected bacteria cleared, compared with over 90% in the bacteria alone group ($p < 0.01$) (Fig. 2B). Coinfusion with CRP (40 μg CRP/20 g b.w.) surprisingly shortens the time by ~25% compared with bacteria alone (IRR 0.75: 95% CI; 0.56, 0.99), with CRP levels below 100 mg/l in mouse blood. However, infusion of more CRP to maintain CRP around 100 mg/l did not significantly alter the time to bacteria clearance (IRR 0.75: 95% CI; 0.52, 1.07) until CRP levels reached 300–400 mg/l, which significantly delayed bacteria clearance compared with bacteria alone (IRR 1.88: 95% CI; 1.34, 2.62) (Fig. 2C). Because human CRP could form complexes with mouse VLDL in vitro and in vivo (Supplemental Fig. 1A), the delay of bacterial clearance by infusion high doses of CRP were most likely caused by high levels of CRP–VLDL complex formation in vivo.

Tissue macrophages take up bacteria and CRP–VLDL complexes

Using the mouse bacteremia model, GFP-expressing BL21 bacteria were injected through the tail vein. After 4 h, blood was taken and the mice were sacrificed. The lungs, kidneys, liver, and spleen were homogenized and the GFP protein was concentrated using anti-GFP agarose beads prior to Western blotting (Fig. 3A). GFP protein was found to be distributed mainly in liver, spleen, and blood (Fig. 3A). CRP–VLDL significantly reduced liver uptake of bacteria to increase the extent of circulating bacteria (Fig. 3B, 3C), without significant changes in spleen uptake (Fig. 3D). In tissue sections, fluorescent bacteria were mainly present in the liver (Fig. 3Eb), with a few in the spleen and lungs, but not in the kidneys or white cells in blood smears. This observation supports previous reports that the liver is the major organ for blood bacterial clearance, at least for *E. coli* (31). When liver sections were stained using anti-CD163 to highlight Kupffer cells (Fig. 3Ea, d, g), as demonstrated in Fig. 3Ea–c, bacteria were taken up by Kupffer cells. Fluorescently labeled CRP–VLDL complexes injected i.v. were also found to be concentrated in Kupffer cells (Fig. 3Ee, f), but fluorescently labeled VLDL alone was barely detectable (Fig. 3Eh, i). This result suggests that tissue macrophages are the major mechanism by which both blood bacteria and CRP–VLDL complexes are cleared and that high extracellular levels of these complexes might delay bacterial clearance by competing for or affecting phagocytosis, particularly by Kupffer cells.

Phagocytosis of E. coli by PMA-activated U937 cells was affected by in vitro–generated and naturally occurring CRP–VLDL complexes

U937 cells induced to differentiate by PMA (32) have been used as in vitro models to study macrophage function (33). Using this model to measure the effects of CRP–VLDL complexes on phagocytosis of bacteria, flow cytometric analysis demonstrated that ~50% of activated U937 cells take up fluorescent bacteria (Fig. 4Aa). Coincubation with isolated VLDL (200 mg/l) had no significant effect on the percentage of cells taking up bacteria (52 ± 10%), but in vitro–generated CRP–VLDL complexes (equal to 40 mg/l CRP and 200 mg/l Apo proteins) significantly reduced these numbers (21 ± 9%, $p < 0.01$) (Fig. 4Ab). CRP alone increased the number of bacteria-containing cells (68 ± 12%, $p < 0.05$), as reported previously (34) (Fig. 4Ac). Addition of human serum to the experimental system (up to 25% of the total reaction volume) demonstrated that those from patients with sepsis, containing naturally occurring CRP–VLDL complexes, showed stronger inhibitory effects on phagocytosis of *E. coli* by activated U937 cells (23 ± 8%) than serum from normal individuals without
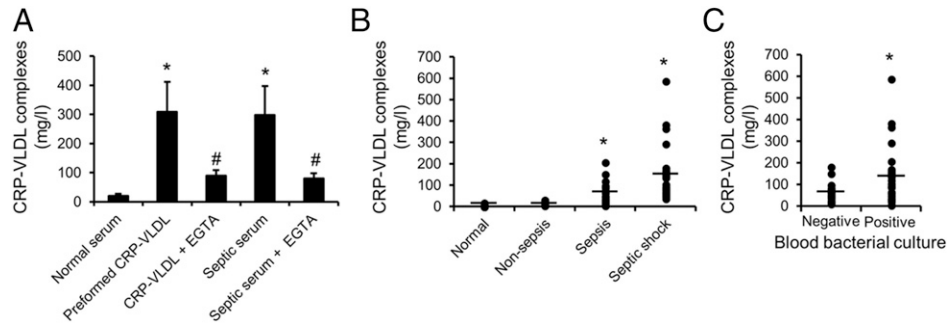
FIGURE 1. CRP–VLDL complexes exist in the circulation of patients with sepsis. (**A**) CRP–VLDL complex ELISA of serum samples from patients with sepsis ($n = 3$) and normal controls ($n = 3$), performed in the presence of 2.5 mM CaCl$_2$. In vitro–generated CRP–VLDL complex was used as a positive control. In some experiments, EGTA (10 mM) was added to samples to chelate calcium and disrupt calcium-dependent CRP–VLDL complexes. CRP–VLDL complexes were quantified as milligrams per liter of lipoprotein. The mean $\pm$ SD from three independent measurements are shown. *$p < 0.01$ when compared with normal serum, #$p < 0.05$ when compared with the same samples without EGTA. (**B**) CRP–VLDL complex ELISA of serum from healthy donors ($n = 20$) and nonseptic ICU ($n = 21$), septic ($n = 21$), and septic shock ($n = 25$) patients. *$p < 0.05$ when compared with healthy donor group. (**C**) CRP–VLDL complex ELISA of septic patients comparing those with positive blood cultures with those whose cultures were negative. *$p = 0.029$.

the complexes ($56 \pm 12\%$, $p < 0.01$) (Fig. 4Ad). To ensure that the flow cytometric results reflected bacteria within rather than adhering to cells, a modified phagocytosis assay using confocal microscopy was established. Fig. 4B shows a typical image for calculating phagocytosis index. The average number of bacteria per cell was measured and a similar result was obtained (Fig. 4C). In vitro–generated CRP–VLDL complexes and sera from septic patients significantly reduced the number of bacteria taken up per cell ($p < 0.05$), whereas CRP alone significantly increased the phagocytosis index ($p < 0.05$). These observations indicate that CRP–VLDL complexes in blood may inhibit phagocytosis of bacteria by tissue macrophages.

Fcγ and scavenger receptors are involved in the uptake of both CRP–VLDL and bacteria by PMA-activated U937 cells

As Fcγ receptors are involved in the phagocytosis of CRP-opsonized bacteria or cells (25), we speculated that CRP-opsonized VLDL may be taken up through a similar mechanism. Based on the aggregative nature of the CRP–VLDL complexes, the scavenger receptors responsible for uptake of modified or aggregated lipoproteins might also be involved. PMA-activated U937 cells expressing Fcγ II (CD32), FcγI (CD64), SA1, and CD36 (a member of scavenger receptor B family) (Fig. 5A) were used to evaluate the roles of these receptors. VLDL uptake by PMA-activated U937 cells was quantified using [^{125}I]-labeled VLDL. To reduce the effect of aggregated VLDL, which may occur during labeling and purification processes, [^{125}I]-labeled VLDL was mixed with VLDL-deficient serum and centrifuged prior to the assay. Activated U937 cells took up VLDL at a rate of $\sim 346 \pm 51$ ng lipoprotein/mg cell protein (mean $\pm$ SD) (Fig. 5B). Once VLDL was mixed with over 200 mg/l CRP, VLDL uptake was significantly increased by over 80% after a 4 h incubation (Fig. 5B) (ANOVA test, $p < 0.05$). This increase was partially inhibited by adding anti-CD32 ($p < 0.05$), anti-CD64 ($p < 0.05$), or anti-CD36 ($p < 0.05$) Abs but not anti-SA1 Ab (Fig. 5C) ($p > 0.05$). This result indicated that both Fcγ receptors and CD36 are involved. However, VLDL uptake in the absence of CRP was not significantly affected by these blocking Abs ($p > 0.05$) (Fig. 5D). Using our modified phagocytosis assay, anti-CD32 and anti-CD64 Abs reduced the rate of phagocytosis significantly ($p < 0.05$) by 66 and 50%, respectively. Anti-CD36 slightly decreased the rate of phagocytosis, but with only borderline significance (Fig. 5E) ($p = 0.09$), whereas the 25% reduction with anti-SA1 was significant ($p < 0.05$). It is therefore likely that CRP–VLDL complexes compete with bacteria for CD-32 and CD-64 receptors to affect bacterial clearance.
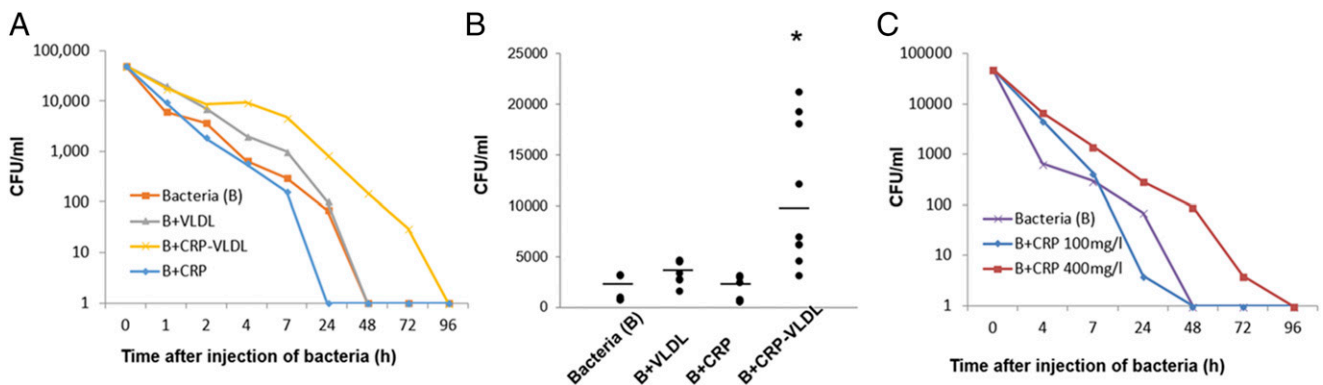
FIGURE 2. Bacterial clearance curves in mice. Mice were injected through the tail vein with 60,000 CFU of overnight cultured BL21 bacteria per 20 g b.w. to achieve $\sim 50,000$ CFU/ml blood, 5 min postinjection. Graph shows mean CFU of time course of blood cultures from at least five mice per group. (**A**) Effect of in vitro–generated CRP–VLDL complexes (200 µl containing; 40 µg CRP + 200 µg VLDL/20 g b.w.) on bacterial clearance. For controls, equal amounts of VLDL or CRP were injected. Total injection volume was no more than 300 µl/20 g b.w. within each 24-h period (estimated to be <30% of total blood volume). Bacteria (**B**) alone: five mice; B+VLDL: seven mice; B+CRP: seven mice; B+CRP–VLDL: 10 mice. (B) Bacterial culture growth of blood 4 h after bacteria injection. Mean CFU in each group is shown. *$p < 0.05$ compared with other groups. (**C**) Effect of 100 or 300–400 mg/l CRP. Highly concentrated CRP was injected before and 4, 9, 14, and 25 h after bacterial injection to maintain concentrations in mouse blood for more than 24 h. Bacteria (**B**) alone: five mice; B+CRP 100 mg: five mice; and B+CRP 400 mg: five mice.
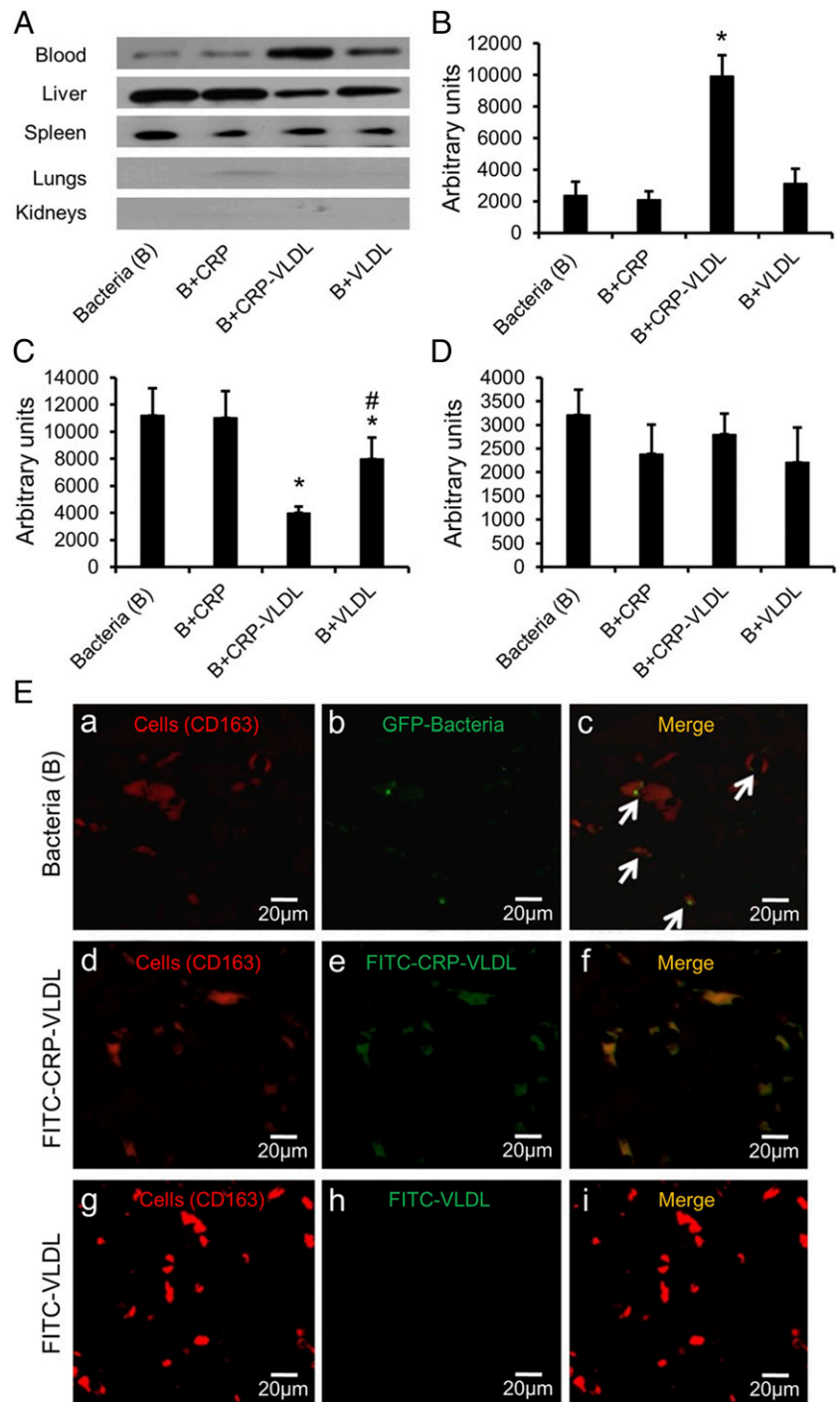
FIGURE 3. Uptake of bacteria and CRP–VLDL complexes by Kupffer cells. (**A**) Western blotting of relative levels of GFP in blood, liver, spleen, lungs, and kidneys of mice 4 h after i.v. injection of GFP-expressing bacteria (B) only and with CRP, CRP–VLDL, or VLDL, respectively, as described in Fig. 2A. (**B–D**) Mean ± SD of the GFP band densities of blood (B), liver (C), and spleen (D) from three independent experiments. *ANOVA test $p < 0.05$ compared with bacteria alone, $^{\#}p = 0.03$ when compared with bacteria + CRR–VLDL. (**E**) Mice were injected i.v. with GFP-expressing bacteria, FITC-labeled VLDL, or CRP-FITC-labeled VLDL complexes and sacrificed after 4 h. (**Ea–c**) Sections from the liver of a mouse injected with GFP–*E. coli*, (a) stained with goat anti-mouse CD163 and anti-goat IgG TRICT conjugate to highlight Kupffer cells, (b) showing presence of GFP-*E.coli* green fluorescence, and (c) merged images of (a) and (b). Arrows point to the GFP-bacteria in the Kupffer cells. (**Ed–f**) Sections from the liver of a mouse injected with CRP-FITC-labeled VLDL complexes, (d) anti-CD163 staining of Kupffer cells, (e) green fluorescence from injected FITC-VLDL, and (f) merged images of (d) and (e). (**Eg–i**) from the liver section of a mouse injected only with FITC-VLDL with (g) anti-CD163 staining of Kupffer cells, (h) green fluorescence from FITC-VLDL, and (i) merged images of (g) and (h). Five mice were used in each treatment group and typical images are presented. Scale bar, 20 μm.

CRP–VLDL complex is mediated by the Pch moiety

The molecular mechanism underlying formation of the CRP–VLDL complexes was investigated so as to explore interruption of CRP–VLDL complexes in functional studies with a view to potential therapeutic strategies. CRP-lipid interactions are calcium dependent and can be affected by Pch. However, as CRP does not bind to all types of lipid vesicles and living cells, there is doubt as to whether this interaction is solely through the hydrophilic head of phosphatidylcholine. Furthermore, apo-E involvement has also been reported (18). Site-directed mutagenesis to evaluate the contribution of the Pch group to the formation of CRP–VLDL complexes was therefore performed, and the critical amino acids E66 and E81 in the Pch binding site of CRP protein (35) were

mutated. T173, which is critical for complement binding on the opposite side of the Pch group binding site (25), was also used as control. These recombinant proteins were individually added to normal serum to a concentration of 300 mg/l and compared with wild-type CRP in their ability to form complexes. The extent of wild-type CRP in forming CRP–VLDL complexes based on reductions in light transmittance (TL18) was assigned a value of 100%, and the relative capacities of E66A, E81A, and T173A mutant proteins were 22, 27, and 95%, respectively (Fig. 6A). The levels of complexes formed with wild-type and mutant CRP were also measured by ELISA with similar results (Supplemental Fig. 1B). E66A or E81A mutation abolished 70–80% of the capacity of CRP to form complexes with VLDL. This confirms that the
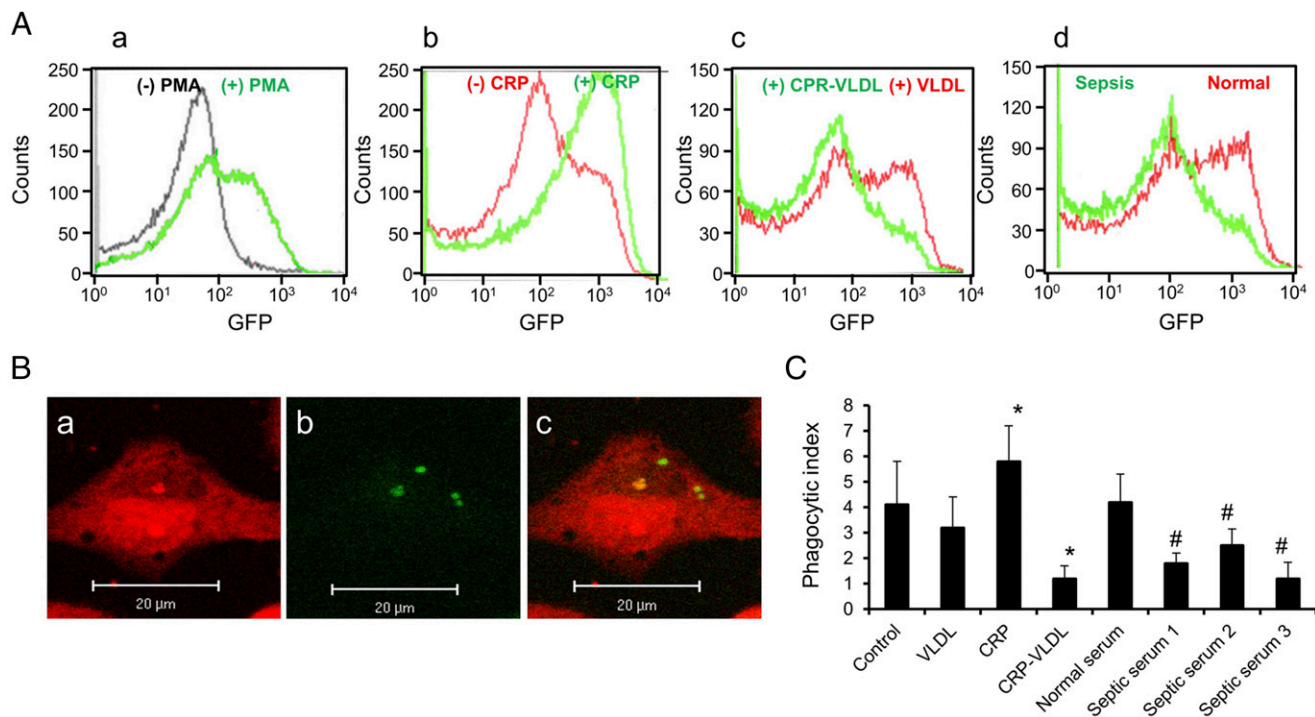
FIGURE 4. CRP–VLDL complex affects phagocytosis. (**A**) Flow cytometric analysis showing (**a**) the effect of PMA activation of U937 cells on bacteria uptake, (**b**) bacteria uptake by PMA-activated U937 cells in the absence (red) or presence of CRP (green), (**c**) the effect of VLDL alone (red) or in complex with CRP (green) on bacterial uptake, and (**d**) the effect of 25% sera from patients with sepsis (green) or normal individuals (red) on bacteria uptake. (**Ba–c**) Modified phagocytosis assay. Typical image of Phagocytosis of fluorescent bacteria by PMA-activated U937 cells. After incubation of PMA-activated U937 cells with GFP-expressing bacteria, cells were washed extensively and stained with propidium iodide, as described in *Materials and Methods*. The green dots are the fluorescent bacteria (GFP), and the red color (propidium iodide) outlines the shape of a cell with a relatively strongly stained nucleus. Scale bar, 20 μm. (**C**) Using this assay with basal media as a control, the effect of CRP (40 mg/l) or VLDL (200 mg/l) alone or in complex (CPR–VLDL) was tested alongside 25% sera from normal controls and serum from three patients with severe sepsis (with aPTT biphasic waveform TL18 results of 72%, 92%, and 67%, respectively). Phagocytosis index were calculated as described in *Materials and Methods*, and mean ± SD were from at least six independent experiments. *$p < 0.05$ compared with control, #$p < 0.05$ compared with normal serum.

interaction of CRP with the Pch moiety is the major mechanism for forming CRP–VLDL complexes.

Pch can efficiently disrupt CRP–VLDL complexes and reverse their inhibitory effects on phagocytosis and blood bacterial clearance

Pch is a natural ligand of CRP and has the strongest affinity among all known interacting partners of CRP (10). Because Pch is small and water soluble, it is an ideal competitor of VLDL for the binding site on CRP. The disrupting effect of Pch was seen from concentrations as low as 10 μM and was nearly maximal at over 500 μM (Fig. 6B). Over 90% of the in vitro–generated complexes could be disrupted by 10 mM Pch (Fig. 6B). CRP–VLDL complex formation in sera from patients with severe sepsis can be easily visualized by the turbidity change following addition of 8 mM CaCl2 (Fig. 6C tube B). Addition of 10 mM Pch prevented this calcium–induced turbidity (Fig. 6C tubes A, C) and also disrupted pre-existing turbidity or preformed complexes (Fig. 6C tube B). Furthermore, complex disruption by Pch was not reversed by increasing the concentration of calcium (Fig. 6D) and signifies that this is not occurring by the same mechanism as EGTA, which chelates Ca^{2+}. When subsequently centrifuged at 14,000 rpm for 10 min, over 90% of the resultant pellet could be redissolved by adding 10 mM Pch. The resultant solution contained CRP and lipoproteins, as determined by mass spectrometry. This result further confirms that the aPTT-induced turbidity changes as profiled through the biphasic waveform is a valid method for detecting aggregated CRP–VLDL complexes.

Pch was also able to abolish the CRP-enhanced uptake of [125I]-labeled VLDL by PMA-activated U937 cells (Fig. 6E). In the phagocytosis assay, Pch reversed nearly 80% of the inhibitory effects of both in vitro–generated and naturally occurring CRP–VLDL complexes (Fig. 6F). In the mouse bacteremia model, addition of Pch to the complex before tail vein injection resulted in dramatic reductions in the levels of CRP–VLDL complexes in blood (Supplemental Fig. 1C–F). Their inhibitory effects on bacterial clearance were also significantly reversed ($p < 0.05$), but clearance was still delayed compared with the response with bacteria alone ($p < 0.05$) (Supplemental Table II), and therefore, use of Pch still requires further optimization to achieve its maximum effect. In general, these data indicate a potential for development of new therapies using Pch or its homologs for septic patients with high levels of CRP–VLDL complexes.

Discussion

The clinical significance of CRP–VLDL complexes was serendipitously discovered through an atypical waveform profile in the aPTT coagulation assay, which turned out to be caused by formation of CRP–VLDL complexes in the plasma of patients with sepsis (21). The diagnostic and prognostic values of the complexes have been validated (22–24, 36, 37), and this strong clinical association, with close correlation to sepsis progression, suggested that CRP–VLDL complexes might have a pathological link to sepsis. Because the biphasic aPTT waveform reflects the induced aggregation of CRP–VLDL complexes by addition of 8 mM CaCl2, an ELISA has now been established to enable direct
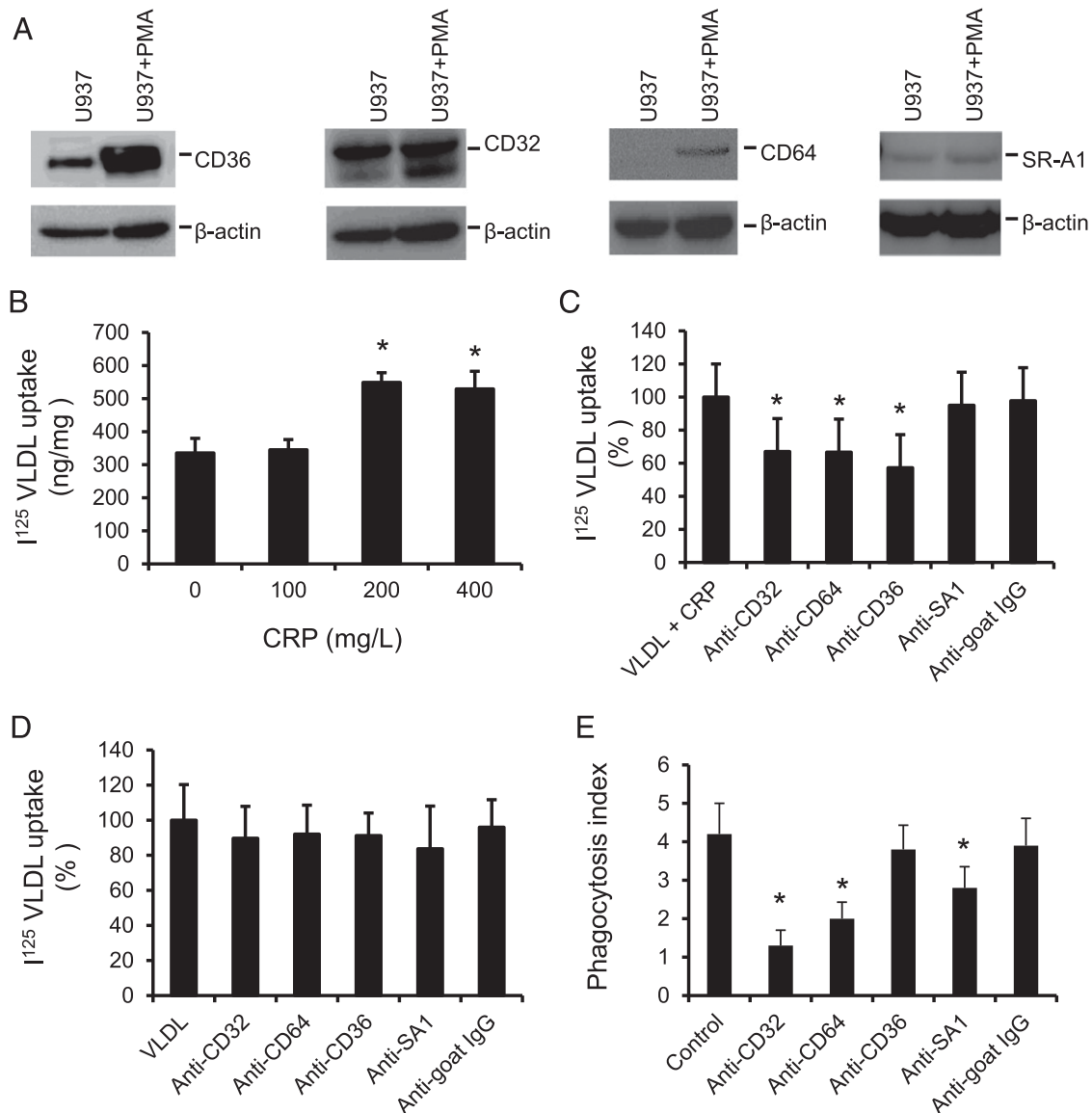
FIGURE 5. Involvement of Fcγ and scavenger receptors in the uptake of both CRP–VLDL complexes and bacteria by activated U937 cells. (**A**) Expression of Fcγ and scavenger receptors in PMA-activated/nonactivated U937 cells. Ten micrograms of cell lysate from nonactivated and activated cells were subjected to Western blotting using anti-CD36, anti-CD32, anti-CD64, and anti-SA1, respectively. β-Actin served as loading control. (**B**) Uptake of soluble [^{125}I] VLDL in VLDL-deficient serum by PMA-activated U937 cells at different CRP concentrations. *$p < 0.01$ from three independent experiments compared with [^{125}I] VLDL alone. (**C**) [^{125}I] VLDL-CRP complex uptake or (**D**) [^{125}I] VLDL uptake in the absence or presence of anti-CD32, anti-CD64, anti-CD36, and anti-SA1blocking Abs with anti-goat IgG isotype as a control. *$p < 0.05$ compared with that without [^{125}I] VLDL + CRP alone. (**E**) The rate of bacteria phagocytosis by PMA-activated U937 cells was assessed in the presence of anti-CD32, anti-CD64, anti-CD36, anti-SA1, and anti-goat IgG isotype control Abs. The mean ± SD from five independent experiments are shown. *$p < 0.05$ compared with control.

detection of circulating CRP–VLDL complexes. The correlation coefficient between the two methods is around −0.6 ($p < 0.01$). CRP complexes with purified VLDL, but not LDL and high density lipoprotein, were detected in the turbidity-based assay (Supplemental Fig. 2A–C). It is generally believed that CRP binding to LDL only occurs upon modification (e.g., by oxidation or immobilization of LDL onto surfaces) (14, 38, 39). Using the ELISA, low levels of CRP–LDL complexes could be detected when CRP was incubated with LDL at equal concentrations to VLDL in the presence of 2.5 mM CaCl$_2$ (Supplemental Fig. 2C). It is not known if the CRP–LDL complexes detected contained modified LDL, but it would appear that circulating CRP–VLDL are predominantly detected by this ELISA.

The association of CRP–VLDL complexes with the severity of sepsis and their significant correlation with blood bacterial culture

positivity suggests the possibility of a role for these complexes in blood bacterial clearance. Using a mouse bacteremia model, i.v. injection of in vitro–generated CRP–VLDL complexes significantly delayed bacterial clearance. Furthermore, addition of Pch to disrupt preformed complexes significantly reduced this inhibitory effect. Consistent with previous reports that Kupffer cells in the liver are the major mechanism for removal of bacteria from blood (31, 40), GFP-labeled bacteria were visualized mainly within Kupffer cells 4 h after i.v. injection. Of interest, infused FITC-labeled VLDL alone was not similarly concentrated in Kupffer cells unless administered in complex with CRP. This would suggest that CRP–VLDL complexes compete with circulating bacteria for clearance by these tissue macrophages. This inhibitory effect by in vitro–generated and naturally occurring CRP–VLDL complexes on bacterial phagocytosis was illustrated using PMA-activated
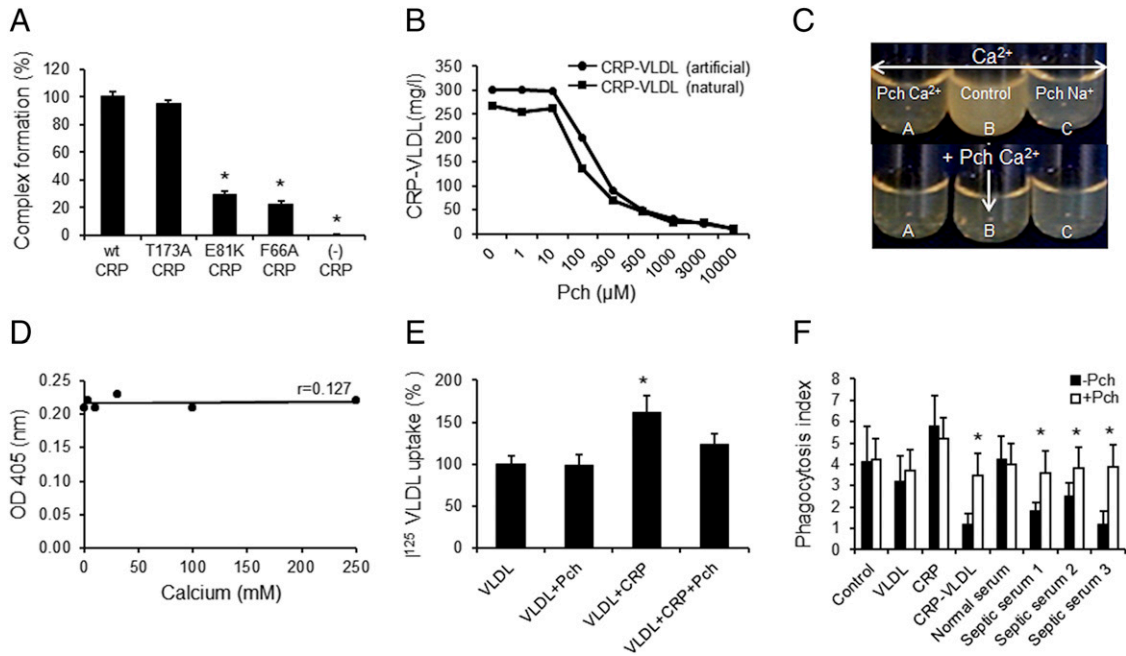
FIGURE 6. Effects of CRP mutants and Pch on CRP–VLDL complex formation. (**A**) The effect of adding 300 mg/l wild-type and mutant CRP proteins (T173A, E81K, and F66A) to normal serum on CRP–VLDL complex formation, as analyzed by aPTT waveform assay. The ability of wild-type (wt) CRP to form the complexes was set at 100% and no CRP [(−) CRP] at 0%. The relative ability (mean ± SD) of each CRP mutant to complex with VLDL in normal serum from five experiments is shown. *$p < 0.05$ compared with wt CRP. (**B**) Effect of 0–10 mM Pch on the complex formation of CRP with isolated VLDL (artificial, ●) or naturally occurring CRP–VLDL complexes (natural, ■) in serum from patients with sepsis. The complexes were measured by ELISA. Averages from three experiments are plotted against the concentration of Pch added. (**C**, upper panel) Serum from a patient with sepsis was aliquoted to test tubes A, B, and C. Pch calcium salt (10 mM), control buffer, and Pch sodium salt (10 mM) were added to test tubes A, B, and C, respectively. Then, CaCl$_2$ was added (8 mM final concentration). (**C**, lower panel) Pch sodium calcium salt (10 mM) was added to test tube B with the precipitate disappearing in a few seconds. (**D**) Turbidity at OD405 nm was measured following the addition of Pch (10 mM). Then, additional CaCl$_2$ (up to 250 mM) was added and the OD405 was determined. Correlation coefficient, $r = 0.127$, $p > 0.05$. (**E**) Effect of Pch (10 mM) on CRP-enhanced uptake of [^{125}I] VLDL by PMA-activated U937 cells. The relative uptake of [^{125}I] VLDL (mean ± SD) in presence of Pch and/or CRP are shown (compared with [^{125}I] VLDL alone, which was set to 100%). *$p = 0.012$ compared with VLDL alone, #$p = 0.038$ compared with VLDL + CRP. (**F**) Effect of Pch (10 mM) on bacterial phagocytosis by activated U937 cells. The mean ± SD phagocytosis index without (■) or with Pch (□) from three experiments are shown. *$p < 0.05$ compared with the same sample without Pch.

U937 cells, whereby complex uptake could be blocked in the presence of Pch, anti-CD32, anti-CD36, and anti-CD64 Abs. These results indicate that Fcγ and scavenger receptors are involved in CRP–VLDL complex uptake, and, because they are also involved in bacterial removal, it is likely that CRP–VLDL complexes inhibit phagocytosis of bacteria by competing for these common receptors. Another possible explanation is that the CRP–VLDL complexes are toxic to recipient cells with consequent reduction in their ability to phagocytose. Such a mechanism of action requires further investigation.

A further finding is that the effect of CRP alone on phagocytosis and blood bacterial clearance can be completely reversed depending on its concentration. CRP was able to increase the phagocytic uptake of BL21 bacteria at concentrations from 100 to 300 mg/l in the absence of serum within the culture medium. This effect was not due to opsonization of bacteria because CRP does not bind to the bacteria and the effect could not be interrupted by Pch. It may be that CRP facilitates phagocytosis through activating Fcγ receptors. This effect was shown in the experimental mouse model whereby 100 mg/l CRP enhanced blood bacterial clearance. In contrast, CRP concentrations above 300 mg/l significantly reduced the efficiency of bacterial clearance. At these concentrations, large amounts of CRP–VLDL complexes were formed within the circulatory system as detected by ELISA (Supplemental Fig. 2C), and the inhibitory effect on blood bacterial clearance was significantly reduced by Pch (Supplemental Table II). These observations suggest that the inhibitory effects on blood bacterial

clearance rely on the high concentrations of circulating CRP–VLDL complexes, which form only when CRP levels increased rapidly and dramatically. This explanation is supported by previous observations that the aPTT biphasic waveform abnormality occurs mainly when CRP levels are over 200 mg/l. In a group of 1187 patients admitted to ICU, 44% of the patients with the aPTT biphasic waveform died compared with 22% of patients without the abnormality (37). Although patients with the aPTT biphasic waveform tend to have very high CRP levels (over 200 mg/l), CRP levels are not well correlated with the degree of the abnormality, as quantified by the light TL18. Furthermore, the aPTT biphasic waveform is a much better predictor of sepsis and mortality than CRP or VLDL alone (23, 37).

Addition of CRP to normal serum also formed CRP–VLDL complexes, which could be detected by aPTT waveform analysis and by ELISA (Supplemental Fig. 2D). Complexes before detectable at CRP levels >100 mg/l and increase to reach a plateau at concentrations of 400 mg/l. This observation could partially answer the discrepancy between clinical observations and animal experiments on the protective or harmful effects of CRP. Clinically, CRP can reach 400–500 mg/l in severe sepsis, and such high levels reflect the severity of the disease and its poor outcome. However, the protective effects of CRP in *Streptococcus pneumoniae* infection or endotoxemia have been demonstrated in the majority of reports using CRP transgenic mice (41, 42) or passive infusion of CRP into mice (43, 44). We also found that CRP could detoxify circulating histones by direct interaction (6). Under those

circumstances, blood CRP levels were around 100 mg/l in the majority of reported cases (41, 42, 45, 46). As such, there would have been insignificant amounts of CRP–VLDL complexes in these animals, and the beneficial effects of CRP would have predominated.

In a cohort of septic patients, the correlation coefficient, r, between circulating CRP levels and aPTT TL18, was -0.63 ($p < 0.01$), and the correlation between CRP and CRP–VLDL complex detected by ELISA was $r = 0.56$ ($p < 0.01$). Although both these correlations are statistically significant, the r values indicate that there was not a strong correlation. Through the investigation of a series of samples from patients with sepsis, we found that in the recovery phase, normalization of aPTT biphasic changes did not rely on clearance of CRP (Supplemental Fig. 2E). In dividing the whole clinical course into an initial phase and a recovery phase separated by the lowest aPTT TL18 value, the correlation between CRP and TL18 was improved in the initial phase (r values from -0.6 to -0.78, $p < 0.05$) but lost significance in the recovery phase ($r = -0.32$, $p > 0.05$). If the levels of CRP in the sera of patients with sepsis as well as in normal controls were adjusted to 300 mg/l by adding CRP, biphasic changes were induced in the initial phase and normal control sera to indicate formation of large amount of complexes. However, addition of 300 mg/l CRP in the recovery phase serum barely produced detectable complexes (Supplemental Fig. 2F). Thus, there may be a natural compensatory mechanism to combat formation of CRP–VLDL complexes, but its precise nature is as yet unclear. Therefore, CRP is not a surrogate marker for CRP–VLDL complexes although high CRP levels are essential for its formation.

As with other studies, use of human CRP in a mouse model can be controversial. This is because the mouse system may not fully represent what happens in humans when high levels of CRP–VLDL complexes are present. However, because CRP is not an acute phase protein in mice, levels of CRP in mouse blood are controllable by giving human or rabbit CRP. In addition, human CRP activates mouse complement (47) and forms complexes with mouse VLDL (Supplemental Fig. 1A). This is therefore an ideal system to monitor the effect of CRP–VLDL complexes on bacterial clearance through the innate immune system. Of importance is the observation that the majority of bacteria were cleared by tissue macrophages (Fig. 3), and this suggests that bacterial killing in blood by activated complement or other factors was not the major route for blood bacterial clearance in this animal model.

In this study, Pch was able to completely disrupt the formation of CRP–VLDL complexes and partially reverse their effects in vitro and in vivo. In contrast to phosphatidylcholine with its hydrophobic fatty acids, Pch is water soluble. Biologically, Pch is an important intermediate in choline metabolism and membrane lipid synthesis. In human blood, Pch levels are around 2 μM, but levels needed to completely disrupt CRP–VLDL complexes in sepsis were found to be between 200 and 500 μM (Fig. 6B). Levels of up to 10 mM are not lethal to mice and they reduce the inhibitory effects of CRP–VLDL complexes on bacterial clearance. As such, Pch and/or its analogs could potentially be used to disrupt CRP–VLDL complexes in sepsis.

Although this study provides a biological basis for the clinical findings of the aPTT waveform in sepsis, a limitation is that phagocytosis and blood clearance were tested in one E. coli strain bacteremia mouse model, which does not mean that organ dysfunction would occur and might therefore not be sufficient for the diagnosis of sepsis in clinical terms. Although the effects of CRP–VLDL on phagocytosis by macrophages are generic, the ability of individual bacterial strains to escape phagocytosis or their toxicity

to macrophages and their proliferation rates are different. The overall effect of CRP–VLDL complexes may therefore vary in different microbial infections and sepsis with different extent of organ failure. In addition, the effects of CRP–VLDL may be different between CRP binding and nonbinding bacterial strains. For example, CRP directly binds and opsonizes *S. pneumoniae* (3, 48), and availability of Pch would enhance the ability of CRP in complement activation (49) but would interfere with opsonization of *S. pneumoniae*. The effect of CRP, CRP–VLDL complexes, and Pch in this infection could therefore be complicated. The differential effects of CRP–VLDL complexes and Pch on individual types of infections will be determined further in future studies.

Disclosures

References

1. Hoesel, L. M., T. A. Neff, S. B. Neff, J. G. Younger, E. W. Olle, H. Gao, M. J. Pianko, K. D. Bernacki, J. V. Sarma, and P. A. Ward. 2005. Harmful and protective roles of neutrophils in sepsis. *Shock* 24: 40–47.
2. Yeh, C. F., C. C. Wu, S. H. Liu, and K. F. Chen. 2019. Comparison of the accuracy of neutrophil CD64, procalcitonin, and C-reactive protein for sepsis identification: a systematic review and meta-analysis. *Ann. Intensive Care* 9: 5.
3. Langereis, J. D., E. S. van der Pasch, and M. I. de Jonge. 2019. Serum IgM and C-reactive protein binding to phosphorylcholine of nontypeable *Haemophilus influenzae* increases complement-mediated killing. *Infect. Immun.* 87: e0029-e19.
4. Yoshinaga, R., Y. Doi, K. Ayukawa, and S. Ishikawa. 2017. High-sensitivity C reactive protein as a predictor of inhospital mortality in patients with cardiovascular disease at an emergency department: a retrospective cohort study. *BMJ Open* 7: e015112.
5. Marnell, L., C. Mold, and T. W. Du Clos. 2005. C-reactive protein: ligands, receptors and role in inflammation. *Clin. Immunol.* 117: 104–111.
6. Abrams, S. T., N. Zhang, C. Dart, S. S. Wang, J. Thachil, Y. Guan, G. Wang, and C. H. Toh. 2013. Human CRP defends against the toxicity of circulating histones. *J. Immunol.* 191: 2495–2502.
7. Liuzzo, G., L. M. Biasucci, J. R. Gallimore, R. L. Grillo, A. G. Rebuzzi, M. B. Pepys, and A. Maseri. 1994. The prognostic value of C-reactive protein and serum amyloid a protein in severe unstable angina. *N. Engl. J. Med.* 331: 417–424.
8. Danesh, J., J. G. Wheeler, G. M. Hirschfield, S. Eda, G. Eiriksdottir, A. Rumley, G. D. Lowe, M. B. Pepys, and V. Gudnason. 2004. C-reactive protein and other circulating markers of inflammation in the prediction of coronary heart disease. *N. Engl. J. Med.* 350: 1387–1397.
9. Casas, J. P., T. Shah, A. D. Hingorani, J. Danesh, and M. B. Pepys. 2008. C-reactive protein and coronary heart disease: a critical review. *J. Intern. Med.* 264: 295–314.
10. Pepys, M. B., G. M. Hirschfield, G. A. Tennent, J. R. Gallimore, M. C. Kahan, V. Bellotti, P. N. Hawkins, R. M. Myers, M. D. Smith, A. Polara, et al. 2006. Targeting C-reactive protein for the treatment of cardiovascular disease. *Nature* 440: 1217–1221.
11. Hirschfield, G. M., J. Herbert, M. C. Kahan, and M. B. Pepys. 2003. Human C-reactive protein does not protect against acute lipopolysaccharide challenge in mice. *J. Immunol.* 171: 6046–6051.
12. Teoh, H., A. Quan, F. Lovren, G. Wang, S. Tirgari, P. E. Szmitko, A. J. Szalai, M. E. Ward, and S. Verma. 2008. Impaired endothelial function in C-reactive protein overexpressing mice. *Atherosclerosis* 201: 318–325.
13. Thompson, D., M. B. Pepys, and S. P. Wood. 1999. The physiological structure of human C-reactive protein and its complex with phosphocholine. *Structure* 7: 169–177.
14. Chang, M. K., C. J. Binder, M. Torzewski, and J. L. Witztum. 2002. C-reactive protein binds to both oxidized LDL and apoptotic cells through recognition of a common ligand: phosphorylcholine of oxidized phospholipids. *Proc. Natl. Acad. Sci. USA* 99: 13043–13048.
15. Singh, U., M. R. Dasu, P. G. Yancey, A. Afify, S. Devaraj, and I. Jialal. 2008. Human C-reactive protein promotes oxidized low density lipoprotein uptake and matrix metalloproteinase-9 release in Wistar rats. *J. Lipid Res.* 49: 1015–1023.
16. Cabana, V. G., H. Gewurz, and J. N. Siegel. 1982. Interaction of very low density lipoproteins (VLDL) with rabbit C-reactive protein. *J. Immunol.* 128: 2342–2348.
17. de Beer, F. C., A. K. Soutar, M. L. Baltz, I. M. Trayner, A. Feinstein, and M. B. Pepys. 1982. Low density lipoprotein and very low density lipoprotein are selectively bound by aggregated C-reactive protein. *J. Exp. Med.* 156: 230–242.

18. Rowe, I. F., A. K. Soutar, I. M. Trayner, G. R. Thompson, and M. B. Pepys. 1984. Circulating human C-reactive protein binds very low density lipoproteins. *Clin. Exp. Immunol.* 58: 237–244.

19. Downey, C., R. Kazmi, and C. H. Toh. 1997. Novel and diagnostically applicable information from optical waveform analysis of blood coagulation in disseminated intravascular coagulation. *Br. J. Haematol.* 98: 68–73.

20. Downey, C., R. Kazmi, and C. H. Toh. 1998. Early identification and prognostic implications in disseminated intravascular coagulation through transmittance waveform analysis. *Thromb. Haemost.* 80: 65–69.

21. Toh, C. H., J. Samis, C. Downey, J. Walker, L. Becker, N. Brufatto, L. Tejidor, G. Jones, W. Houdijk, A. Giles, et al. 2002. Biphasic transmittance waveform in the APTT coagulation assay is due to the formation of a Ca(++)-dependent complex of C-reactive protein with very-low-density lipoprotein and is a novel marker of impending disseminated intravascular coagulation. *Blood* 100: 2522–2529.

22. Chopin, N., B. Floccard, F. Sobas, J. Illinger, E. Boselli, F. Benatir, A. Levrat, C. Guillaume, J. Crozon, C. Négrier, and B. Allaouchiche. 2006. Activated partial thromboplastin time waveform analysis: a new tool to detect infection? *Crit. Care Med.* 34: 1654–1660.

23. Dempfle, C. E., S. Lorenz, M. Smolinski, M. Wurst, S. West, W. P. Houdijk, M. Quintel, and M. Borggrefe. 2004. Utility of activated partial thromboplastin time waveform analysis for identification of sepsis and overt disseminated intravascular coagulation in patients admitted to a surgical intensive care unit. *Crit. Care Med.* 32: 520–524.

24. Zakariah, A. N., S. M. Cozzi, M. Van Nuffelen, C. M. Clausi, O. Pradier, and J. L. Vincent. 2008. Combination of biphasic transmittance waveform with blood procalcitonin levels for diagnosis of sepsis in acutely ill patients. *Crit. Care Med.* 36: 1507–1512.

25. Bang, R., L. Marnell, C. Mold, M. P. Stein, K. T. Clos, C. Chivington-Buck, and T. W. Clos. 2005. Analysis of binding sites in human C-reactive protein for FcgammaRI, FcgammaRIIA, and C1q by site-directed mutagenesis. *J. Biol. Chem.* 280: 25095–25102.

26. Bodman-Smith, K. B., A. J. Melendez, I. Campbell, P. T. Harrison, J. M. Allen, and J. G. Raynes. 2002. C-reactive protein-mediated phagocytosis and phospholipase D signalling through the high-affinity receptor for immunoglobulin G (FcgammaRI). *Immunology* 107: 252–260.

27. Aderem, A., and D. M. Underhill. 1999. Mechanisms of phagocytosis in macrophages. *Annu. Rev. Immunol.* 17: 593–623.

28. Plüddemann, A., C. Neyen, and S. Gordon. 2007. Macrophage scavenger receptors and host-derived ligands. *Methods* 43: 207–217.

29. Bone, R. C., W. J. Sibbald, and C. L. Sprung. 1992. The ACCP-SCCM consensus conference on sepsis and organ failure. *Chest* 101: 1481–1483.

30. Wang, G., A. Ma, C. M. Chow, D. Horsley, N. R. Brown, I. G. Cowell, and P. B. Singh. 2000. Conservation of heterochromatin protein 1 function. *Mol. Cell. Biol.* 20: 6970–6983.

31. Klein, A., M. Zhadkewich, J. Margolick, J. Winkelstein, and G. Bulkley. 1994. Quantitative discrimination of hepatic reticuloendothelial clearance and phagocytic killing. *J. Leukoc. Biol.* 55: 248–252.

32. Rovera, G., D. Santoli, and C. Damsky. 1979. Human promyelocytic leukemia cells in culture differentiate into macrophage-like cells when treated with a phorbol diester. *Proc. Natl. Acad. Sci. USA* 76: 2779–2783.

33. Whyte, J., A. D. Roberts, K. A. Morley, R. J. Sharp, and P. D. Marsh. 2000. Phagocytosis of mycobacteria by U937 cells: a rapid method for monitoring uptake and separating phagocytosed and free bacteria by magnetic beads. *Lett. Appl. Microbiol.* 30: 90–94.

34. Casey, R., J. Newcombe, J. McFadden, and K. B. Bodman-Smith. 2008. The acute-phase reactant C-reactive protein binds to phosphorylcholine-expressing *Neisseria meningitidis* and increases uptake by human phagocytes. *Infect. Immun.* 76: 1298–1304.

35. Agrawal, A., S. Lee, M. Carson, S. V. Narayana, T. J. Greenhough, and J. E. Volanakis. 1997. Site-directed mutagenesis of the phosphocholine-binding site of human C-reactive protein: role of Thr76 and Trp67. *J. Immunol.* 158: 345–350.

36. Toh, C. H., and A. R. Giles. 2002. Waveform analysis of clotting test optical profiles in the diagnosis and management of disseminated intravascular coagulation (DIC). *Clin. Lab. Haematol.* 24: 321–327.

37. Toh, C. H., L. O. Ticknor, C. Downey, A. R. Giles, R. C. Paton, and R. Wenstone. 2003. Early identification of sepsis and mortality risks through simple, rapid clot-waveform analysis. Implications of lipoprotein-complexed C reactive protein formation. *Intensive Care Med.* 29: 55–61.

38. Tabuchi, M., K. Inoue, H. Usui-Kataoka, K. Kobayashi, M. Teramoto, K. Takasugi, K. Shikata, M. Yamamura, K. Ando, K. Nishida, et al. 2007. The association of C-reactive protein with an oxidative metabolite of LDL and its implication in atherosclerosis. *J. Lipid Res.* 48: 768–781.

39. Matsuura, E., G. R. Hughes, and M. A. Khamashta. 2008. Oxidation of LDL and its clinical implication. *Autoimmun. Rev.* 7: 558–566.

40. Naito, M., G. Hasegawa, Y. Ebe, and T. Yamamoto. 2004. Differentiation and function of Kupffer cells. *Med. Electron Microsc.* 37: 16–28.

41. Szalai, A. J., D. E. Briles, and J. E. Volanakis. 1995. Human C-reactive protein is protective against fatal *Streptococcus pneumoniae* infection in transgenic mice. *J. Immunol.* 155: 2557–2563.

42. Xia, D., and D. Samols. 1997. Transgenic mice expressing rabbit C-reactive protein are resistant to endotoxemia. *Proc. Natl. Acad. Sci. USA* 94: 2575–2580.

43. Nakayama, S., H. Gewurz, T. Holzer, T. W. Du Clos, and C. Mold. 1983. The role of the spleen in the protective effect of C-reactive protein in *Streptococcus pneumoniae* infection. *Clin. Exp. Immunol.* 54: 319–326.

44. Mold, C., T. W. Du Clos, S. Nakayama, K. M. Edwards, and H. Gewurz. 1982. C-reactive protein reactivity with complement and effects on phagocytosis. *Ann. N. Y. Acad. Sci.* 389: 251–262.

45. Mold, C., B. Rodic-Polic, and T. W. Du Clos. 2002. Protection from *Streptococcus pneumoniae* infection by C-reactive protein and natural antibody requires complement but not Fc gamma receptors. *J. Immunol.* 168: 6375–6381.

46. Suresh, M. V., S. K. Singh, D. A. Ferguson, Jr., and A. Agrawal. 2007. Human C-reactive protein protects mice from *Streptococcus pneumoniae* infection without binding to pneumococcal C-polysaccharide. *J. Immunol.* 178: 1158–1163.

47. Suresh, M. V., S. K. Singh, D. A. Ferguson, Jr., and A. Agrawal. 2006. Role of the property of C-reactive protein to activate the classical pathway of complement in protecting mice from pneumococcal infection. *J. Immunol.* 176: 4369–4374.

48. Mold, C., C. P. Rodgers, R. L. Kaplan, and H. Gewurz. 1982. Binding of human C-reactive protein to bacteria. *Infect. Immun.* 38: 392–395.

49. Mold, C., H. Gewurz, and T. W. Du Clos. 1999. Regulation of complement activation by C-reactive protein. *Immunopharmacology* 42: 23–30.

Key Points

- Kupffer cells phagocytose both bacteria and CRP–VLDL complexes.
- High levels of CRP–VLDL complexes delay bacterial clearance.
- Pch disrupts CRP–VLDL complexes to improve bacterial clearance.